ApJ Submitted: Accepted:

The Anglo-Australian Planet Search – XX. A Solitary Ice-giant Planet Orbiting HD 102365[1]

C. G. Tinney[2], R. Paul Butler[3], Hugh R. A. Jones[4], Robert A. Wittenmyer[2] Simon O'Toole[5], Jeremy Bailey[2], Brad D. Carter[6]

c.tinney@unsw.edu.au

ABSTRACT

We present 12 years of precision Doppler data for the G3 star HD 102365, which reveals the presence of a Neptune-like planet with a 16.0 M_{Earth} minimum mass in a 122.1 d orbit. Very few "Super Earth" planets have been discovered to date in orbits this large, and those that have been found reside in multiple systems of between three and six planets. HD 102365b, in contrast, appears to orbit its star in splendid isolation. Analysis of the residuals to our Keplerian fit for HD 102365b indicates that there are no other planets with minimum mass above 0.3 M_{Jup} orbiting within 5 AU and no other "Super Earths" more massive than 10 M_{Earth} orbiting at periods shorter than 50 d. At periods of less than 20 d these limits drop to as low as 6 M_{Earth}. There are now 32 exoplanets known with minimum mass below 20 M_{Earth}, and interestingly the period distributions of these low-mass planets seem to be similar whether they orbit M-, K- or G-type dwarfs.

Subject headings: planetary systems – stars: individual (HD 102365)

1. Introduction

In recent years, extending the threshold for exoplanet detection to yet lower and lower masses has been a significant endeavour for exoplanetary science. As at 2010 October, thirty-one exoplanets

[1]Based on observations obtained at the Anglo-Australian Telescope, Siding Spring, Australia.

[2]Department of Astrophysics, School of Physics, University of New South Wales, NSW 2052, Australia

[3]Department of Terrestrial Magnetism, Carnegie Institution of Washington, 5241 Broad Branch Road NW, Washington D.C. USA 20015-1305

[4]Centre for Astrophysical Research, University of Hertfordshire, Hatfield, AL10 9AB, UK

[5]Australian Astronomical Observatory, P.O. Box 296, Epping, NSW 1710, Australia

[6]Faculty of Sciences, University of Southern Queensland, Toowoomba, Queensland 4350, Australia

have been published with minimum (i.e. $m \sin i$) masses of less than $20\,M_{\rm Earth}$. All have been found in orbits of less than a few hundred days, corresponding to orbital radii of $\lesssim 1$ AU. Roughly equal numbers have been found orbiting M-, K- and G-type dwarfs (10, 11 and 10 respectively in each of these spectral types). This roughly equal distribution hides several selection effects. First that finding very low-mass planets orbiting G-dwarfs is *much* harder than finding them orbiting M-dwarfs, since the lower mass of an M-dwarf primary will (for a given mass planet with a given orbital period) make the Doppler amplitude of an M-dwarf exoplanet at least three times larger than a G-dwarf one. And second, that current planet search target lists are dominated by G-dwarfs.

The detection of such low-mass exoplanets has in large part been due to the dramatic improvements achieved in the intrinsic, internal measurement precisions of Doppler planet search facilities. These have improved to such an extent that noise sources *intrinsic* to the parent star are the major limiting factor for very low-mass exoplanet detection. Characterisation of these noise sources (jitter, convective granulation and asteroseismological p-mode oscillations) has become an important focus of Doppler planet detection. A few obvious modifications to current observing strategies have emerged – (1) target low-mass stars; (2) target chromospherically inactive and slowly rotating stars; (3) target high-gravity stars (where p-mode oscillations are minimised) and (4) extend the observations of stars over several p-mode fundamental periods, so that asteroseismological noise is suppressed.

The Anglo-Australian Planet Search began operation in 1998 January, and is currently surveying 250 stars. It has first discovered 33 exoplanets with $m \sin i$ ranging from $5.1\,M_{\rm Earth}$to $10\,M_{\rm Jup}$ (Tinney et al. 2001, 2002, 2003, 2005, 2006; Butler et al. 2001, 2002; Jones et al. 2002, 2003a,b, 2006, 2010; Carter et al. 2003; McCarthy et al. 2004; O'Toole et al. 2007, 2009; Bailey et al. 2009; Vogt et al. 2010a). Over the last 5 years, each of the observing strategy improvements listed above have been implemented in this planet search program, resulting in the detection of several low-amplitude systems in recent years (e.g. 61 Vir bcd, HD 16417b - Vogt et al. 2010a; O'Toole et al. 2009). In this paper, we add to this track record, with the discovery of a $16\,M_{\rm Earth}$ planet in a 122.1 ± 0.3 d orbit around the G3 star HD 102365.

2. HD 102365

HD 102365 (Gl 442A, HIP 57443, LHS 311) lies at a distance of 9.24 ± 0.06 pc (Perryman et al. 1997), and has been classified as both a G3V (Keenan & McNeil 1989) and a G5V (Evans et al. 1957). It has an absolute magnitude of $M_{\rm V} = 5.06$ ($V = 4.89$) and $B - V = 0.664$. Hipparcos photometry finds it to be photometrically stable at the 4 milli-magnitude level over 112 observations over the course of the Hipparcos mission (Perryman et al. 1997).

HD 102365 was identified by Van Biesbrock (1961) as being a member of a common-proper-motion binary system. Its companion star (LHS 313, Gl 442B) is considerably fainter (V=15.43). Hawley et al. (1996) identified the companion as an M4V, and it was recovered by 2MASS at a

position angle and separation consistent with the earlier identification, had optical-near-infrared colours consistent with being a binary companion to HD 102365. Its near-infrared photometry (M_J=8.8±0.2) indicates a mass of 0.2 $M_\odot$ (using the mass-luminosity relations of Delfosse et al. 2000). The separation of the components on the sky corresponds to a distance of 322 AU, which would place the orbital period of the companion in the region of tens of thousands of years.

HD 102365 is a bright, nearby and Sun-like star. It has therefore been the subject of multiple atmospheric and isochronal analyses – the conclusions reached by the most recent of these are summarised in Table 1. In brief, HD 102365 is ≈100 K cooler than the Sun, has a metallicity a factor of two lower (i.e. −0.3 dex), and a mass about 15% lower. In the analysis which follows we assume a mass of 0.85$M_\odot$.

HD 102365 is also a very slow rotator ($v \sin i$ =0.7 km s^{-1}) and inactive (with a mean R'_{HK} from the two published measurements of −4.99). Its predicted stellar jitter due to activity is 2.1 m s^{-1} (using the updated Ca II jitter calibration of J.Wright (priv.comm.)). Asteroseismology will also contribute jitter to observations of HD 102365, however this impact will be small at less than a 0.14 m s^{-1} rms noise equivalent (for observations of more than 10 minutes) using the relations of O'Toole et al. (2008).

3. Observations

Anglo-Australian Planet Search (AAPS) Doppler measurements are made with the UCLES echelle spectrograph (Diego et al. 1990). An iodine absorption cell provides wavelength calibration from 5000 to 6200 Å. The spectrograph point-spread function and wavelength calibration is derived from the iodine absorption lines embedded on every pixel of the spectrum by the cell (Valenti et al. 1995; Butler et al. 1996).

Observations of HD 102365 began as part of the AAPS main program in 1998 January, and over the following seven years it was observed regularly in observations of 200-400s (depending on observing conditions) giving a signal-to-noise ratio (SNR) of ≈200 per spectral pixel in the iodine region. These are the observations listed in Table 2 between JD=2450830.212-2453402.195. In 2005 April, HD 102365 (together with a number of other bright AAPS targets) was elevated within our observing program to high-SNR status, such that its target SNR per epoch became 400 per spectral pixel. As a result the median internal uncertainties produced by our Doppler fitting process dropped from 1.55 m s^{-1} to 0.89 m s^{-1}. The Doppler velocities derived from all these observations are listed in Table 2.

4. Analysis

The root-mean-square (rms) scatter about the mean velocity of all AAPS data for HD 102365 is 3.0 $\mathrm{m\,s^{-1}}$, which is higher by $\approx 1\,\mathrm{m\,s^{-1}}$ than would be expected based on measurement precision and stellar jitter alone.

Figure 1 shows a Two Dimensional Keplerian Lomb-Scargle periodogram (2DKLS, O'Toole et al. 2007) of these data. The 2DKLS extends the concept of the traditional LS periodogram by fitting Keplerians to the data as a function of period and eccentricity, and allows the identification of an indicated eccentricity (e) as well as an indicated period (P) from a time series of Doppler velocities. The HD 102365 data display an extremely strong peak at a period of 122 d in the two dimensional 2DKLS plane (Fig. 1 upper panel) with the period peak showing no strong dependence on eccentricity, but with a detectable maximum at e=0.36. The power spectrum is shown as a one dimensional spectrum at e=0.36 in the lower panel of the figure. 1.

Figure 2 (upper panel) shows a traditional Lomb-Scargle (LS) periodogram (Lomb 1976; Scargle 1982) for this data set, along with estimated False Alarm Probability limits overlain at 0.1, 1 & 10 % as generated by the Systemic Console code (Meschiari et al. 2009). The 122 d peak appears at a time-scale considerably longer than would be expected if it were associated with the rotation period of this star, which even though a slow rotator ($v \sin i$ =0.7 $\mathrm{m\,s^{-1}}$) is nonetheless predicted to have a rotation period of ∼40 d on the basis of its low chromospheric activity (Noyes et al. 1984).

A least-squares Keplerian fit to the data using the 2DKLS peak as an initial estimate results in the orbital parameters shown in Table 3. Figure 3 displays this fit (and the residuals to it) as a function of orbital phase. The rms scatter to this fit is 2.5$\mathrm{m\,s^{-1}}$, and the reduced chi-squared (χ^2_ν) is 1.08. This fit indicates the presence of a planet with period 122.1±0.3 d, eccentricity 0.34±0.14, semi-major axis 0.46±0.04 AU and minimum mass ($m \sin i$) 16.0±2.6 $\mathrm{M_{Earth}}$.

To test the probability that the noise in our data might have resulted in a false detection, we have run simulations using the "scrambled velocity" approach of Marcy et al. (2005). This technique makes the null hypothesis that no planet is present, and then uses the actual data as the best available proxy for the combined noise due to our observing system and the star. Multiple realisations are created by scrambling the observed velocities amongst the observed epochs. We created 5000 of these scrambled velocity sets, and then subjected them to the same analysis as our actual data set (i.e. identifying the strongest peak in the 2DKLS followed by a least-squares Keplerian fit). No trial amongst 5000 showed a χ^2_ν better than that obtained for the original data set, and the distribution of the scrambled reduced χ^2_ν (see Fig. 4) shows a clear separation from that obtained with the actual data. We conclude that there is a less than 0.02% probability of us having obtained a false detection due to a fortuitous selection from a system with no planet.

Figure 2 (lower panel) shows the power spectrum of the residuals to the AAPS velocities with the fitted Keplerian removed, along with recalculated False Alarm Probabilities at 10, 1, and 0.1%. No other significant periodicities are present in the data once the 122 d planetary signal is removed.

5. Discussion

The planet HD 102365b has a Neptune-like minimum-mass ($m \sin i$=16.0±2.6 M_{Earth}) and moves in an orbit equivalent to the Mercury-Venus region of the inner Solar System, with a periastron of 0.30 AU (c.f. Mercury orbits from 0.307 AU to 0.466 AU) and an apastron of 0.61 AU (Venus orbits from 0.718 AU to 0.728 AU). This places it in a very small group of sub-20 M_{Earth} planets to have been detected at orbital periods beyond that of Mercury – just three such planets have been detected by precision Doppler planet searches to date. They are: Gl 876e ($m \sin i$=14.6 M_{Earth}, P=124.3 d, primary is M4 with 0.32$M_{\odot}$ – Laughlin et al. 2005); HD 69830d ($m \sin i$=18 M_{Earth}, P=197 d, primary is K0 with 0.86$M_{\odot}$ – Lovis et al. 2004); and Gl 581f ($m \sin i$=7.0 M_{Earth}, P=433 d, primary is M3 with 0.31$M_{\odot}$ – Bonfils et al. 2005; Vogt et al. 2010b). Two of these planets orbit much lower-mass M-dwarfs (Gl 876e & Gl 581f), while HD 69830 orbits a K0 dwarf estimated to have a similar mass to that of HD 102365.

Table 4 lists the 32 radial velocity exoplanets currently known with minimum masses less than 20 M_{Earth} (including HD 102365b) and the Figure 5 shows their period distribution. There is a noticeable "pile-up" of such planets at periods of just less than 10 days, which is primarily an understandable result of two selection effects. First, since Doppler amplitude is a strong function of orbital period, planets of a given mass will be more readily detectable at short-periods, than at long periods. And second, detecting planets at very short-periods (i.e. less than 2 days) is very hard in typical Doppler survey data sets, due to the strong aliasing imposed by the diurnal observing pattern. These two effects conspire to produce a peak in exoplanet detectability at 4-10 d for very low-mass exoplanets.

What *is* interesting to note is that the period distribution is very similar for M-, K- and G-type dwarf primaries. Given that these correspond to a variation in typical primary mass of a factor of 3 (and also presumably of the mass of the protoplanetary disk from which these planets formed), this would suggest that the process of forming sub-Neptune mass planets – and then migrating them in to radii of less than 0.6 AU – is not a strong function of stellar or disk mass.

The three planets noted above with similar properties to HD 102365b (Gl 876e, HD 69830d & Gl 581f) *all* lie in multiple systems. The HD 69830 system is a triple, while the two M dwarfs (Gl 876 and Gl 581) host four and six exoplanets, respectively. In contrast, our HD 102365 data show no evidence for additional planets (see Fig. 2). We computed the detectability of additional planets in the residuals to our 1-planet fit, using the method of Wittenmyer et al. (2006, 2010). In brief, we add a Keplerian signal to the existing velocity data, then attempt to recover that signal using a Lomb-Scargle periodogram. The mass of the simulated planet is increased until 99% of the injected signals are recovered with FAP<0.1%. The results of this analysis are shown for $P < 300$ days in Figure 6. Averaged over periods of less than 400 days (corresponding to $a < 1$ AU), our data exclude the presence of planets in circular orbits down to a Doppler amplitude of $K = 1.8 \pm 0.4$ m s^{-1}; that is, there are no "Super Earth" exoplanets more massive than 10 M_{Earth} orbiting at periods of less than 50 d in the HD 102365 system, and no planets more massive than

$20\,M_{Earth}$ within 1 AU. Furthermore, our data rule out all planets with $m \sin i > 0.3\,M_{Jup}$ within 5 AU (corresponding to the 12.4 yr duration of these observations). The HD 102365 system really does appear to contain just one ice giant planet. It would be tempting to attribute the paucity of additional planets in this system to HD 102365's low metallicity of [Fe/H]=−0.30, and a resultant paucity of refractory elements for the formation of cores onto which planetary accretion can take place (Laughlin et al. 2004; Ida & Lin 2004, 2005), were it not for the similarly lower than solar metallicity of Gl 581 (though it must be acknowledged the determining metallicities for M dwarfs is currently problematic, with estimates for these systems varying by as much as 0.3 dex between different authors).

We also note that with a mass smaller than that of the Sun ($0.85 M_{\odot}$), the habitable zone for HD 102365 will lie at smaller orbital radii than it does for the Sun. For an Earth-like planet, Kasting et al. (1993) estimate the habitable zone for a $0.85 M_{\odot}$ star to lie in the range 0.6-1.0 AU. Obviously, HD 102365 is *not* an Earth-like planet, and so such an estimate is not appropriate to the planet itself, which will have very different atmospheric properties to those assumed by Kasting et al. (1993). On the other hand, those assumptions *could* be valid for rocky satellites of HD 102365b, if they exist. Unfortunately, HD 102365b only approaches the inner edge of this habitable zone when near its apastron, and so any satellites are likely to be "uninhabitable" for much of the planet's 122 d eccentric orbit.

We acknowledge support from the following grants; NSF AST-9988087, NASA NAG5-12182, PPARC/STFC PP/C000552/1, ARC Discovery DP774000; and travel support from the Carnegie Institution of Washington and the Australian Astronomical Observatory (formerly the Anglo-Australian Observatory). We are extremely grateful for the extraordinary support we have received from the AAT technical staff – E. Penny, R. Paterson, D. Stafford, F. Freeman, S. Lee, J. Pogson, S. James, J. Stevenson, K. Fiegert, T. Young, G. Kitley, Y. Kondrat and G. Schaffer.

AAT

REFERENCES

Bailey, J.A., Butler, R.P., Tinney, C.G., Jones, H.R.A., O'Toole, S.J. Carter, B.D. & Marcy, G.W. 2009, ApJ, 690, 743

Bond, J.C., Tinney, C. G., Butler, P. R., Jones, H. R. A., Marcy, G. W., Penny, Alan J. & Carter, B. D., 2006, MNRAS, 370, 163

Bouchy, F. et al. 2008, A&A, 496, 527

Bonfils, X. et al. 2005, A&A, 443, L15

Bonfils, X. et al. 2007, A&A, 474, 293

Butler, R. P., Marcy, G. W., Williams, E., McCarthy, C., Dosanjh, P., & Vogt, S. S. 1996, PASP, 108, 500

Butler, R. P., Tinney, C. G., Marcy, G. W., Jones, H. R. A., Penny, A. J. & Apps, K. 2001, ApJ, 555, 410.

Butler, R.P. et al. 2002, ApJ, 578, 565

Butler, R. P. et al. 2006, ApJ, 646, 505

Carter, B.D. et al., 2003, ApJ, 593, L43

Delfosse, X. Forveille, T. Sgransan, D. Beuzit, J.-L. Udry, S. Perrier, C. & Mayor, M. 2000, A&A, 364, 217

Diego, F., Charalambous, A., Fish, A. C., & Walker, D. D. 1990, Proc. Soc. Photo-Opt. Instr. Eng., 1235, 562

Evans, D.S., Menzies, A. & Stoy, R.H. 1957, MNRAS, 117, 534

Fischer, D. A. et al. 2008, ApJ, 675, 790

Forveille, T. et al. 2009, A&A, 493, 645

Gray, R.O. et al., 2006, AJ, 132, 161

Hawley, S. L., Gizis, J.E. & Reid, I. N. 1996, AJ, 112, 2799

Hébrard, G. et al. 2010, A&A, 512, 46

Henry, T. J, Soderblom, D. R., Donahue, R. A. & Baliunas, S. L. 1996, AJ, 111, 439

Holmberg, J., Nordström, B. & Andersen, J. 2009, A&A, 501, 941

Howard, A. et al. 2009, ApJ, 696, 75

Howard, A. et al. 2010, ApJ, submitted, arXiv:1003.3444

Ida S. & Lin, D. N. C. 2004, ApJ, 604, 388

Ida, S. & Lin, D. N. C. 2005, ApJ, 626, 1045

Jones, H.R.A., Butler, R.P., Marcy, G.W., Tinney, C.G., Penny, A.J., McCarthy, C. & Carter, B.D. 2002, MNRAS, 333, 871

Jones, H.R.A., Butler, R.P., Marcy, G.W., Tinney, C.G., Penny, A.J., McCarthy, C. & Carter, B.D. 2003a, MNRAS, 337, 1170

Jones, H.R.A., Butler, R.P., Marcy, G.W., Tinney, C.G., Penny, A.J., McCarthy, C., Carter, B.D. & Pourbaix, D. 2003b, MNRAS, 341, 948

Jones, H.R.A. et al. 2006, MNRAS, 369, 249

Jones, H.R.A. et al. 2010, MNRAS, 403, 1703

Keenan, P.C. & McNeil, R.C. 1989, ApJS, 71, 245

Kasting, J.F., Whitmire, D.P. & Reynolds, R.T. 1993, Icarus, 101, 108

Laughlin, G. and Bodenheimer, P. and Adams, F. C. 2004, ApJ, , 612, L73.

Laughlin, G., Butler, R. P., Fischer, D. A., Marcy, G. W., Vogt, S. S. & Wolf, A. S. 2005, ApJ, 622,1182

Lo Curto, G. et al. 2010, A&A, 512, L48

Lomb, N.R. 1976, Ap&SS, 39, 447

Lovis, C. et al. 2004, Nature, 441, 305

Lovis, C. et al. 2010, A&A, submitted

McArthur, B.E. et al. 2004, ApJ, 614, L81

McCarthy, C. et al, 2004, ApJ, 617, 575

Marcy, G. W. et al. 2005, ApJ, 619, 570

Mayor, M. et al. 2009a, A&A, 493, 639

Mayor, M. et al. 2009b, A&A, 507, 487

Meschiari, S., Wolf, A. S., Rivera, E., Laughlin, G., Vogt, S. & Butler, P. 2009, PASP, 121, 1016

Mordasini, C. et al. 2010, A&A, in press, arXiv:1010.0856v1

Noyes, R. W., Hartmann, L. W., Baliunas, S. L., Duncan, D. K. & Vaughan, A. H. 1984, ApJ, 279, 763

O'Toole, S., et al. 2007, ApJ, 660, 1636

O'Toole, S., Tinney, C.G., Jones, H.R.A. 2008, 386, 516.

O'Toole, S. et al. 2009, ApJ, 697, 1263

Pepe, F. et al. 2007, A&A, 462, 769

Perryman, M. A. C., et al. 1997, A&A, 323, L49. The Hipparcos Catalog

Rivera, E. J. et al. 2005, ApJ, 634, 625

Rivera, E. J., Butler, R. P., Vogt, S.S., Laughlin, G., Henry, G. W. & Meschiari, S. 2010a, ApJ, 708, 1492

Rivera, E. J., Laughlin, G., Butler, R. P., Vogt, S.S., Haghighipour, N. & Meschiari, S. 2010b, ApJ, 719, 890

Santos, N.C. et al. 2004, A&A, 426, L19

Sousa S.G. et al. 2008, A&A, 487, 373

Scargle, J.D., 1982, ApJ, 263, 835

Schröder, C., Reiners, A. & Schmitt, J. H. M. M., 2009, A&A, 493, 1099

Takeda, G., Ford, E.B., Sills, A., Rasio, F.A., Fischer, D.A. & Valenti, J.A. 2007, ApJS, 168, 297

Tinney, C.G., Butler, R.P., Marcy, G.W., Jones, H.R.A., Penny, A.J., McCarthy, C. & Carter, B.D. 2002, ApJ, 571, 528

Tinney, C.G., et al. 2001, ApJ, 551, 507

Tinney, C.G., et al. 2003, ApJ, 587, 423

Tinney, C.G., et al. 2005, ApJ, 623, 1171

Tinney, C.G., et al. 2006, ApJ, 647, 594

Valenti, J. A., Butler, R. P. & Marcy, G. W. 1995, PASP, 107, 966.

Udry, S. et al. 2006, A&A, 447, 361

Udry, S. et al. 2007, A&A, 469, L43

Valenti, J.A. & Fischer, D.A., 2005, ApJS, 159, 141

Van Biesbrock, G. 1951, AJ, 66, 528

Vogt, S.S. et al. 2005, ApJ, 632, 638

Vogt, S.S. et al. 2010a, ApJ, 708, 1366

Vogt, S.S., Butler, R. P., Rivera, E. J., Haghighipour, N., Henry, G. W. & Williamson, M. H. 2010b, ApJ, in press (arXiv:1009.5733)

Wittenmyer, R. A., Endl, M., Cochran, W. D., Hatzes, A. P., Walker, G. A. H., Yang, S. L. S., & Paulson, D. B. 2006, AJ, 132, 177

Wittenmyer, R. A., et al. 2010, ApJ, 722, 1854

Wright, J. T., Upadhyay, S., Marcy, G. W., Fischer, D. A., Ford, E. B., Johnson, J. A. 2009, ApJ, 693, 1084

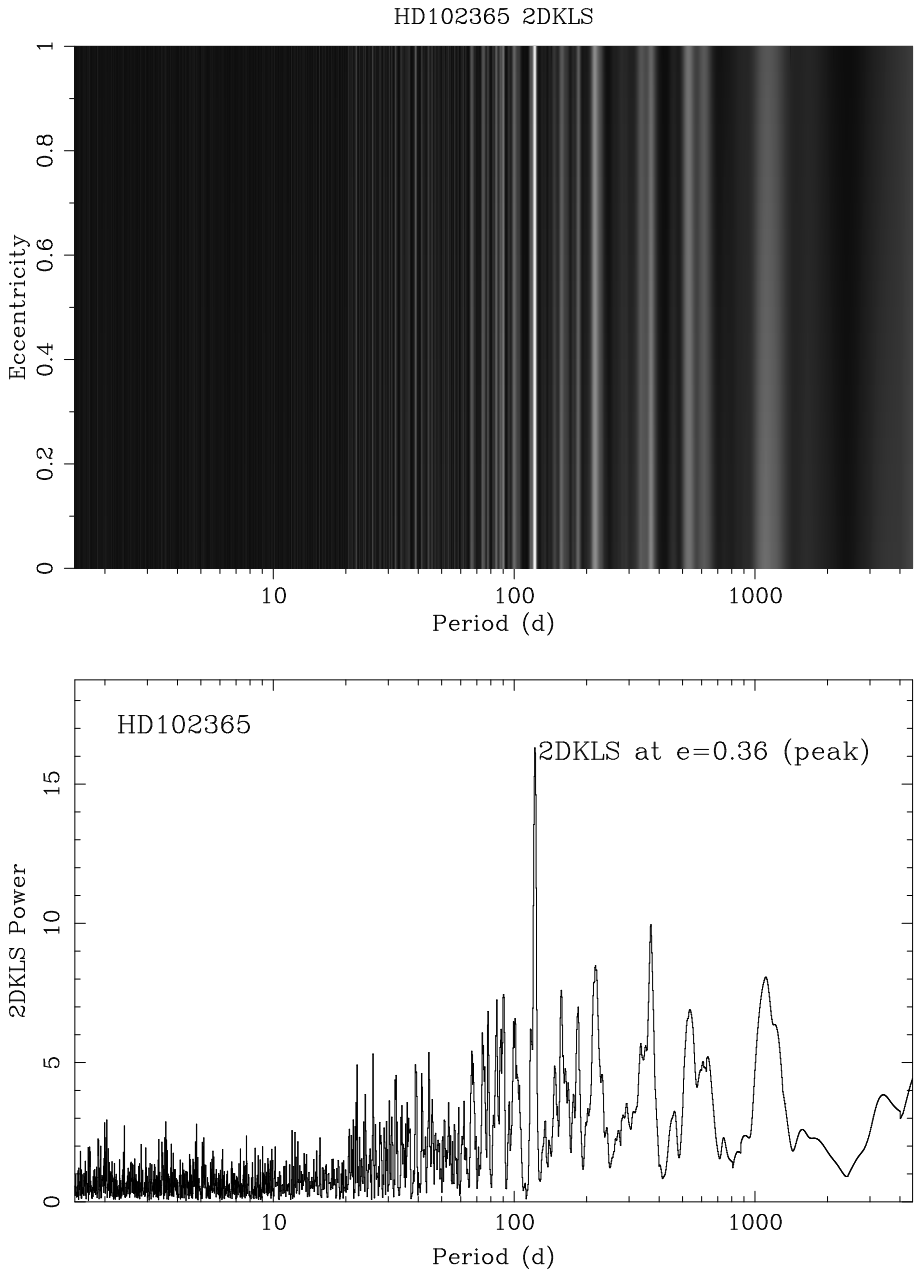

Fig. 1.— 2DKLS Periodograms for HD 102365. *Upper panel* shows the periodic power as a function of assumed planet eccentricity and period. *Lower panel* shows a cut through the 2DKLS at e=0.36 (the location of the peak power in the upper panel).

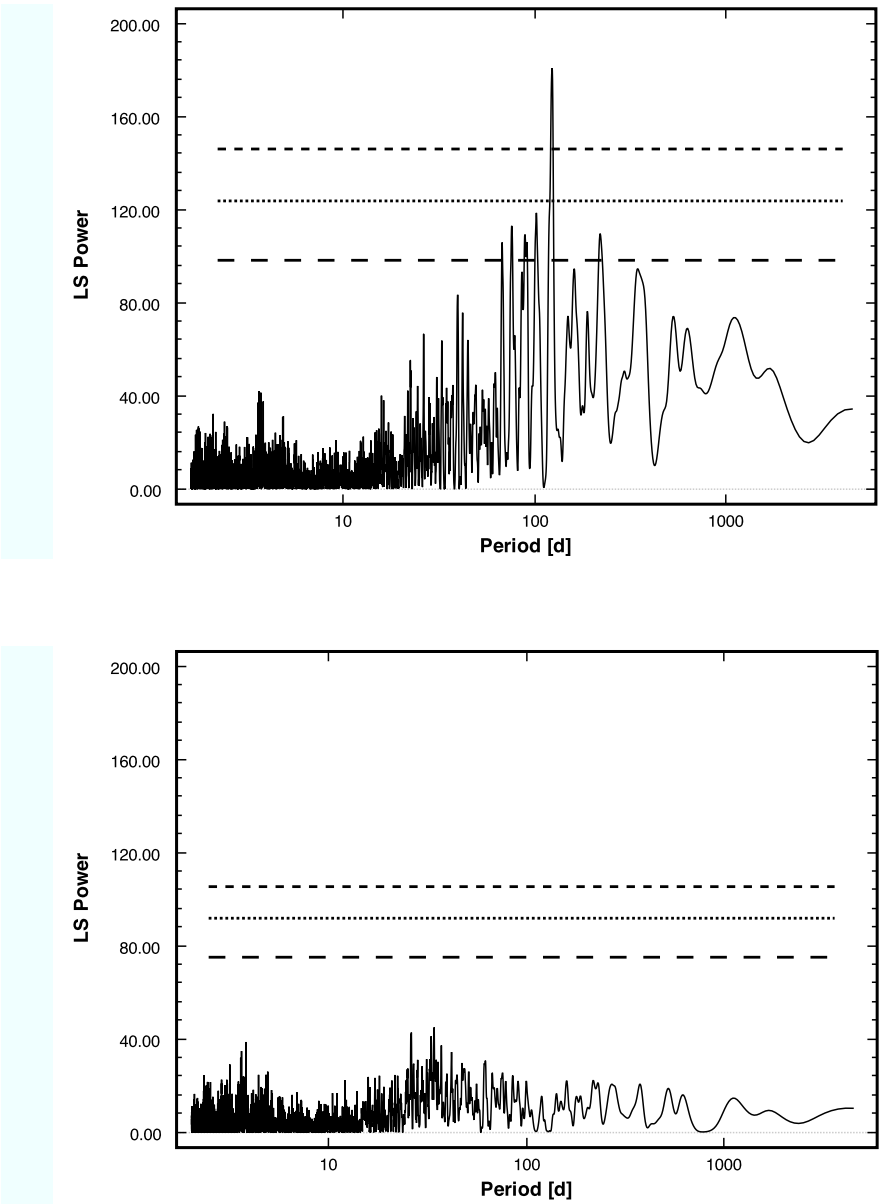

Fig. 2.— Traditional LS Periodograms for HD 102365. *Upper panel* with the false alarm probability levels of 10, 1 and 0.1%. *Lower panel* the same data with the fitted planet removed, and the false alarm probability levels of 10, 1 and 0.1% recalculated. No significant signal is detectable due to a further planet.

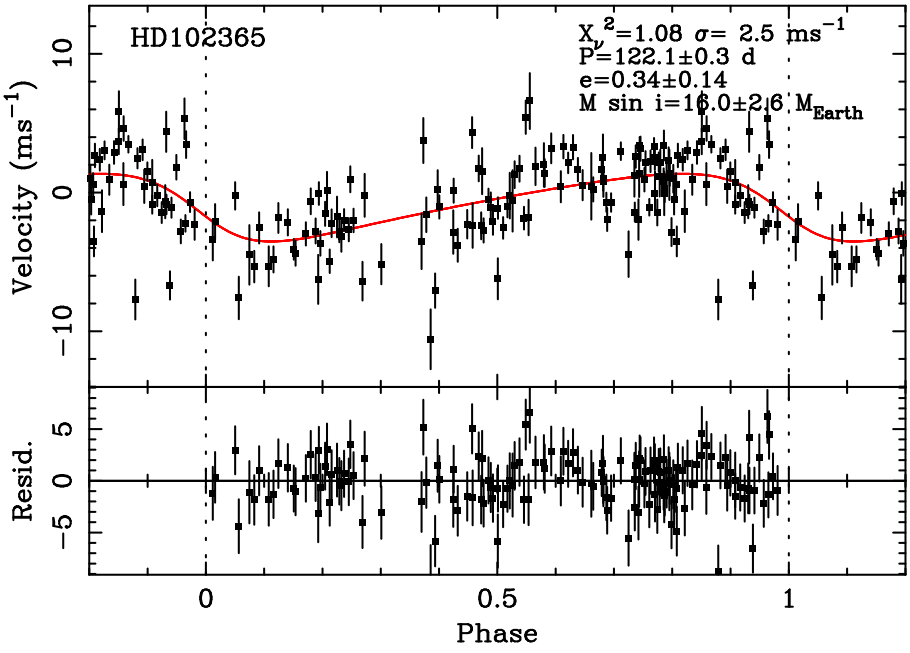

Fig. 3.— Keplerian best fit to Doppler data for HD 102365 phased at the best-fit period. The lower panel shows the residuals to the fit. A host star mass of 0.85 $M_\odot$ and an intrinsic stellar Doppler variability (i.e. jitter) of 2.1 m s^{-1} are assumed

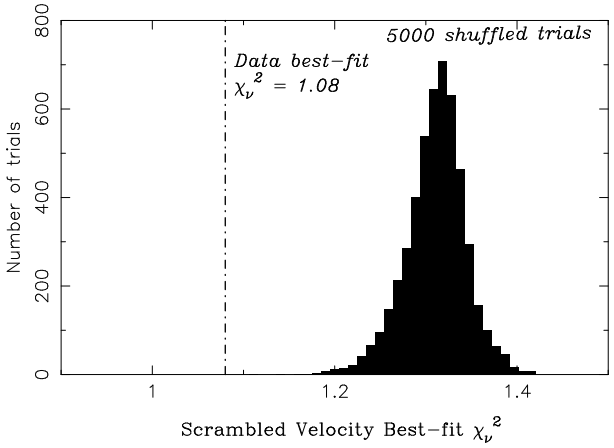

Fig. 4.— Scrambled false alarm probability results. The histogram shows the χ^2_ν values that result from the best Keplerian fits to 5000 realisations of scrambled versions of the AAPS velocities for HD 102365. The dashed line shows the reduced χ^2_ν for our actual data.

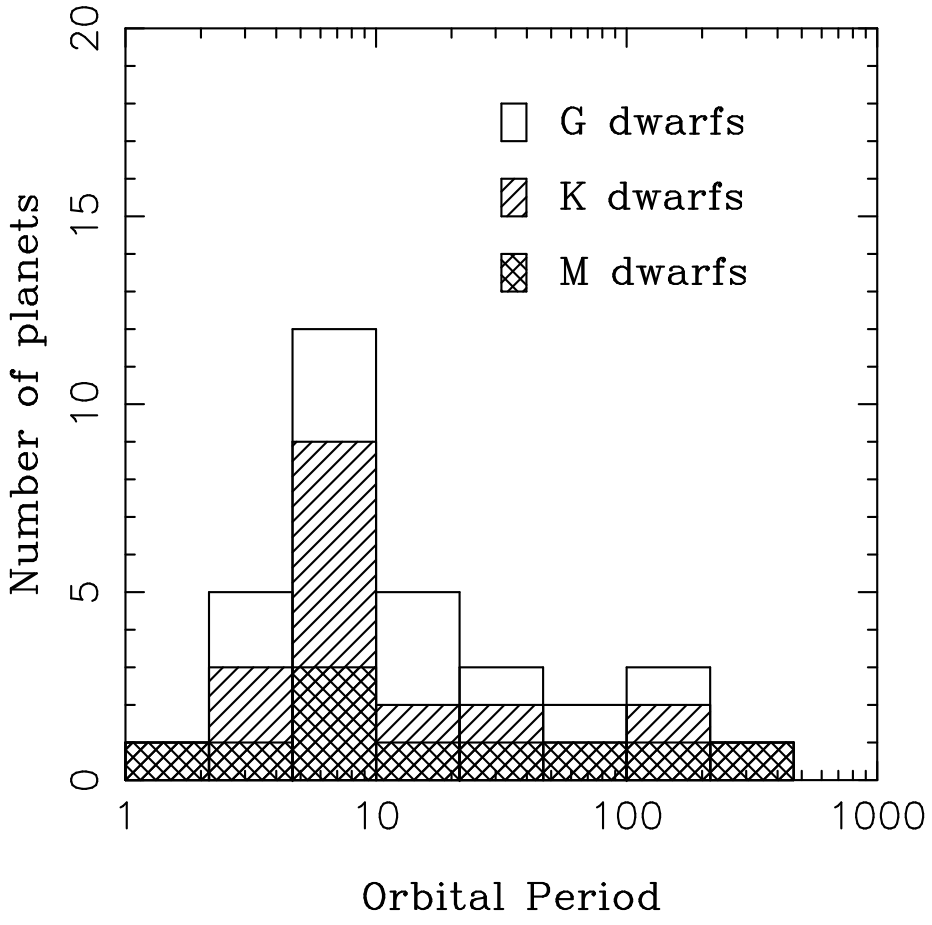

Fig. 5.— Period distribution for the 32 exoplanets currently known with minimum mass $m \sin i < 20\,\mathrm{M_{Earth}}$ (including HD 102365b).

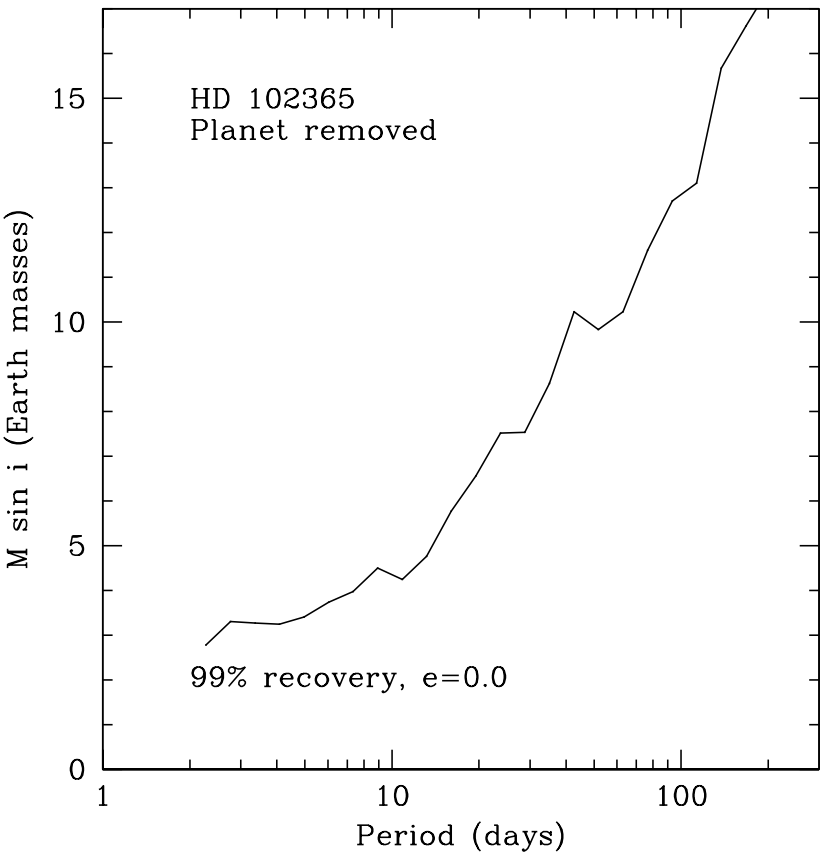

Fig. 6.— Detection limits (at 99% confidence level) for the presence of additional planets in the residuals to our one-planet fit for HD 102365b.

Table 1. Properties of HD 102365

Reference	T_{eff}	[Fe/H]	Mass	log(g)	Age	$v \sin i$	R'_{HK}
Valenti & Fischer (2005); Takeda et al. (2007)[a]	5630 K	−0.26	0.89±0.03$M_\odot$	4.57	9±3 Gyr[1]	0.7 km s^{-1}	···
Sousa et al. (2008)	5629±29 K[b]	−0.29±0.02	0.82$M_\odot$	4.44±0.02	···	···	···
Holmberg et al. (2009)	5650 K	−0.33	···	···	···	···	···
Gray et al. (2006)	5688 K	−0.33	···	4.51	···	···	···
Bond et al. (2006)	5688±100 K	−0.28±0.07	···	4.7±0.2	···	···	···
Schröder et al. (2009)	···	···	···	···	···	···	-5.03
Henry et al. (1996)	···	···	···	···	···	···	-4.95

[a]Mass and age from Takeda et al. (2007), remaining parameters from Valenti & Fischer (2005)

[b]T_{eff} from infrared flux method

Table 2. Velocities for HD 102365

JD (−2450000)	RV ($m\,s^{-1}$)	Uncertainty ($m\,s^{-1}$)	JD (−2450000)	RV ($m\,s^{-1}$)	Uncertainty ($m\,s^{-1}$)	JD (−2450000)	RV ($m\,s^{-1}$)	Uncertainty ($m\,s^{-1}$)
830.2120	−1.95	1.46	3517.8765	+2.14	0.85	4146.1494	+1.52	0.66
970.8882	+0.45	1.20	3518.9348	+2.26	0.78	4147.1817	−0.86	0.66
1213.2263	−7.71	1.44	3519.8345	+2.54	0.91	4148.2115	−0.21	0.78
1237.1088	−4.49	2.15	3520.9700	+2.15	0.94	4149.1503	−1.44	0.76
1274.1669	−1.60	1.25	3521.9180	+0.27	0.95	4150.1458	−0.86	0.70
1275.0686	−10.58	2.16	3522.9518	+1.36	0.87	4151.1931	−1.09	0.73
1382.9017	−6.39	1.40	3568.8441	−2.98	0.84	4152.2082	+1.83	0.89
1631.0427	−5.16	1.45	3569.8610	−0.63	0.93	4153.1592	−2.80	0.86
1682.8377	−4.44	1.65	3570.8839	−2.77	0.90	4154.1097	−2.22	0.60
1684.0503	+1.24	1.53	3571.8931	−3.66	0.89	4155.0789	−0.69	0.72
1717.8540	−3.41	1.48	3572.8653	−1.53	0.87	4156.0537	−2.32	1.09
1743.8680	−1.76	1.47	3573.8496	−4.95	0.85	4222.0454	−0.22	1.65
1919.2349	+0.45	2.40	3575.8540	−2.77	0.82	4223.0693	+1.29	0.97
1984.1277	−6.26	1.77	3576.8510	−1.98	0.79	4224.0894	+1.72	0.94
2009.1581	+0.22	1.39	3577.8470	−2.68	0.84	4225.0363	−1.85	0.82
2060.9266	−1.34	1.51	3578.8456	−2.01	0.85	4226.0030	−1.80	1.28
2127.8671	−3.53	1.99	3700.2461	+0.96	0.94	4252.9565	−1.44	0.93
2388.0430	−6.22	1.48	3753.2481	+0.78	1.09	4254.9066	+1.08	1.00
2420.9725	−0.04	1.55	3840.1183	−7.07	1.24	4255.9285	−2.85	1.01
2421.9764	+1.17	1.45	3841.0030	−1.04	0.84	4257.0523	−3.52	1.08
2422.9051	−0.06	1.57	3844.0169	+0.14	0.87	4543.1122	−4.10	0.75
2423.9770	+1.28	1.82	3937.8743	−0.07	0.82	4550.0793	+0.13	1.36
2424.9796	−0.47	1.11	4038.2472	−2.10	1.27	4551.0414	−2.21	1.00
2455.8883	−7.60	1.53	4111.1843	+3.31	0.85	4553.0691	−3.15	1.12
2654.2716	+2.56	1.63	4112.1940	+2.14	0.74	4841.2280	+3.19	1.08
2745.0216	−2.85	1.57	4113.2161	+3.27	0.88	4843.2598	+0.42	1.12
2749.0801	−2.38	1.61	4114.2235	+1.65	0.85	4897.1422	−0.24	0.99
2751.0742	+1.54	1.66	4115.2295	+0.53	1.09	4901.1335	−5.34	1.14
2783.9628	+1.35	1.67	4119.2316	+1.64	0.82	4902.1479	−2.55	1.12
2860.8442	+3.75	1.62	4120.1772	−0.70	0.69	4904.1774	−5.32	1.44
3005.2531	+6.60	2.02	4121.1826	−0.72	0.67	4905.1780	−4.82	0.94
3008.2151	+1.99	1.58	4123.2074	+2.98	0.64	4906.1968	−1.83	1.08
3041.2850	+5.84	1.47	4126.1448	−1.41	0.69	4908.1785	−2.15	0.95
3042.2136	+0.61	1.52	4127.1543	+3.39	0.62	5031.8906	−4.38	0.90
3048.2584	+0.72	1.63	4128.1690	+0.93	0.85	5202.1955	+5.43	1.20
3051.1885	+4.38	1.45	4129.1708	−1.06	0.60	5204.2366	+1.89	1.35
3214.8709	−0.20	1.55	4130.1644	+3.29	0.65	5206.1761	+1.41	1.00

Table 2—Continued

JD (−2450000)	RV ($m\,s^{-1}$)	Uncertainty ($m\,s^{-1}$)	JD (−2450000)	RV ($m\,s^{-1}$)	Uncertainty ($m\,s^{-1}$)	JD (−2450000)	RV ($m\,s^{-1}$)	Uncertainty ($m\,s^{-1}$)
3245.8512	−0.60	2.21	4131.1706	+2.19	0.70	5231.1466	+3.39	1.08
3402.1950	+0.58	0.82	4132.1780	+0.83	0.92	5253.1614	+3.46	0.97
3482.9418	+1.74	0.93	4133.2403	+2.29	0.97	5310.0451	−3.80	1.19
3483.9734	−2.73	0.87	4134.2021	+1.00	1.00	5312.0515	−2.28	1.03
3485.0087	−0.47	0.75	4135.1689	+2.68	0.85	5313.0652	+4.32	1.12
3485.9286	−2.12	0.93	4136.1870	+2.37	0.79	5314.9743	−2.40	0.97
3486.9909	−1.12	0.78	4137.1852	+3.04	0.65	5316.9911	−1.10	1.11
3488.0592	−2.55	0.78	4138.1656	+0.92	1.09	5370.8847	−0.66	1.20
3488.9752	−1.02	0.77	4139.1564	+2.89	0.82	5371.8836	−6.70	1.02
3506.9189	+0.23	0.87	4140.1589	+3.69	0.93	5374.9315	+5.32	1.47
3509.0173	+0.99	0.86	4141.1830	+4.62	0.89	···	···	···
3509.8462	−1.94	0.83	4142.1777	+3.48	0.60	···	···	···
3515.8545	+2.60	0.81	4144.0637	+2.47	0.73	···	···	···
3516.8477	+3.16	0.87	4145.1442	+3.08	0.75	···	···	···

Table 3. Orbital Solution for HD 102365b

Parameter	Value	Uncertainty
Orbital period P (days)	122.1	0.3
Velocity semiamplitude K ($m\,s^{-1}$)	2.40	0.35
ω (degrees)	105	22
Eccentricity e	0.34	0.14
Periastron date (JD−2450000)	129	11
$m \sin i$ ($M_{\rm Earth}$)	16.0	2.6
Semi-major axis (AU)	0.46	0.04
$N_{\rm fit}$	149	
RMS ($m\,s^{-1}$)	2.5	

Table 4. Exoplanets with Minimum Mass below $20M_{Earth}$

Planet	Mass (M_{Earth})	SpT	Period (d)	Orbit Ref.	Discovery Ref.
Gl 581 e	1.9	M3	3.14	Vogt et al. (2010b)	Mayor et al. (2009b)
Gl 581 g	3.1	M3	36.65	Vogt et al. (2010b)	Vogt et al. (2010b)
HD 156668 b	4.1	K3	4.64	Howard et al. (2010)	Howard et al. (2010)
HD 40307 b	4.2	K2.5	4.31	Mayor et al. (2009a)	Mayor et al. (2009a)
61 Vir b	5.0	G5	4.21	Vogt et al. (2010a)	Vogt et al. (2010a)
Gl 581 c	5.6	M3	12.92	Vogt et al. (2010b)	Udry et al. (2007)
HD 215497 b	6.6	K3	3.93	Lo Curto et al. (2010)	Lo Curto et al. (2010)
Gl 876 d	6.8	M4	1.94	Rivera et al. (2010a)	Rivera et al. (2005)
HD 40307 c	6.9	K2.5	9.62	Mayor et al. (2009a)	Mayor et al. (2009a)
Gl 581 d	5.6	M3	66.9	Vogt et al. (2010b)	Udry et al. (2007)
Gl 581 f	7.0	M3	433	Vogt et al. (2010b)	Vogt et al. (2010b)
HD 181433 b	7.5	K3	9.37	Bouchy et al. (2005)	Bouchy et al. (2005)
HD 1461 b	7.4	G0	5.77	Rivera et al. (2010a)	Rivera et al. (2010a)
55 Cnc e	8.0	G8	2.80	Fischer et al. (2008)	McArthur et al. (2004)
Gl 176 b	8.4	M2.5	8.78	Forveille et al. (2009)	Forveille et al. (2009)
HD 40307 d	9.2	K2.5	20.46	Mayor et al. (2009a)	Mayor et al. (2009a)
HD 7924 b	9.3	K0	5.40	Howard et al. (2009)	Howard et al. (2009)
HD 69830 b	10.2	K0	8.67	Lovis et al. (2004)	Lovis et al. (2004)
μ Ara d[a]	10.5	G3	9.63	Pepe et al. (2007)	Santos et al. (2004)
HD 10180 d	11.9	G1	16.36	Lovis et al. (2010)	Lovis et al. (2010)
GJ 674 b	11.1	M2.5	4.69	Bonfils et al. (2007)	Bonfils et al. (2007)
HD 69830 c	11.8	K0	31.6	Lovis et al. (2004)	Lovis et al. (2004)
HD 4308 b	12.8	G5	15.56	Udry et al. (2006)	Udry et al. (2006)
HD 10180 c	13.2	G1	5.76	Lovis et al. (2010)	Lovis et al. (2010)
BD-08 2823 b	14.4	K3	5.60	Hébrard et al. (2010)	Hébrard et al. (2010)
Gl 876 e	14.6	M4	124.3	Rivera et al. (2010a)	Rivera et al. (2010a)
Gl 581 b	15.6	M3	5.36	Vogt et al. (2010b)	Bonfils et al. (2005)
HD 102365 b	16.0	G3	122	This paper	This paper
HD 90156 b	18.0	G5	49.77	Mordasini et al. (2010)	Mordasini et al. (2010)
HD 190360 c	18.1	G6	17.11	Wright et al. (2009)	Vogt et al. (2005)
HD 69830 d	18.1	K0V	197	Lovis et al. (2004)	Lovis et al. (2004)
61 Vir c	18.2	G5	38.02	Vogt et al. (2010a)	Vogt et al. (2010a)

[a]This is the planet that Pepe et al. (2007) & Santos et al. (2004) refer to as HD 160691 c.